Morphometric Analysis of Human Peripapillary Retinal Nerve Fiber Layer Thickness

Matan J. Cohen, Ehud Kaliner, Shahar Frenkel, Michael Kogan, Hagai Miron, and Eytan Z. Blumenthal

Purpose. The peripapillary retinal nerve fiber layer (RNFL) thickness pattern in the normal human eye has been well characterized using data obtained with scanning laser polarimetry and optical coherence tomography. The authors sought to characterize the normative peripapillary RNFL thickness and pattern using histologic sections obtained from healthy postmortem human eyes.

Methods. Seventeen unpaired normal postmortem eyes were recruited into this study. Each eye was sectioned using the "umbrella technique" to obtain four concentric peripapillary rings, each centered on the optic disc, with diameters of 3.0, 3.5, 4.0, and 4.5 mm. RNFL thickness data along each ring section was measured at 100 equidistant locations. Thickness data, for each ring diameter, across all eyes were averaged to arrive at normative thickness values for the peripapillary RNFL thickness in eyes processed using this technique.

Results. Average RNFL thicknesses (±SD) for the 3.5-mm diameter ring were as follows: overall, 60.3 ± 19.5 μm; superior, 75.3 ± 26.5 μm; inferior, 69.4 ± 22.4 μm; nasal, 48.1 ± 15 μm; temporal, 49.2 ± 26.4 μm. Qualitatively, the RNFL thickness showed a double-hump pattern with relatively similar superior and inferior peaks and with temporal and nasal troughs. Progressively larger peripapillary rings showed progressively thinner RNFL thickness at all quadrants. In contrast, the relative thickness percentage for each quadrant remained unchanged among the four different diameter rings.

Conclusions. Histologic data from a group of healthy postmortem eyes demonstrate the pattern of RNFL thickness in normal eyes. These data corroborate imaging findings of peripapillary RNFL thickness patterns obtained using commercially available RNFL imaging devices. (*Invest Ophthalmol Vis Sci.* 2008;49:941–944) DOI:10.1167/iovs.07-0621

In healthy eyes, the peripapillary RNFL thickness pattern around the optic disc shows a unique pattern, with two peaks (superior and inferior) and two troughs (temporal and nasal).[1] Significant variability exists among healthy persons, as evident by the scatter seen in the normative range plots of two imaging devices (Stratus OCT and GDx-VCC; Carl Zeiss Meditec Inc., Dublin, CA; Fig. 1). The graphical representation of the circumpapillary RNFL thickness is often referred to as a temporal-superior-nasal-inferior-temporal (TSNIT) graph and is classically described as a "double-hump" pattern.[2] The shape the RNFL thickness pattern assumes, as apparent in the TSNIT graph, is referred to as the RNFL thickness modulation around the optic disc.

Much of what we know about RNFL modulation in the human eye is derived from in vivo imaging studies, primarily using scanning laser polarimetry (SLP) and optical coherence tomography (OCT). In addition, few histologic studies have been performed on humans[3,4] and primates.[5–8] However, the data presented in these studies are insufficient to validate the data derived from imaging devices[1] because of the few measurement points obtained for each processed eye and the different histologic approaches used in each of these studies.

In this study, histologic data in the form of 100 equidistant data points collected at four concentric peripapillary diameters were used to plot the modulation of the RNFL thickness pattern in normal human postmortem eyes.

Methods

Globes

Seventeen unpaired human eyes were obtained for research purposes from an eye bank. A detailed postmortem history was obtained in which known eye diseases, previous eye surgery, chronic eye medications, or diabetes and other systemic diseases that may affect retinal morphology were excluded. Macroscopic examination of these eyes excluded gross disease. The eyes were fixed in 4% buffered formaldehyde 5.8 ± 1.9 (range, 3–10.5) hours after death. Consent for the use of tissues in medical research was obtained from the immediate family. Tissue harvesting was performed according to the regulations for obtaining and handling of human tissue for research purposes and in accordance with the tenets of the Declaration of Helsinki for research involving human subjects. Approval for this study was obtained from the Institutional Human Subject Committee.

Tissue Processing and RNFL Thickness Measurements

The technique for sectioning the globe was previously described.[9] Briefly, this "umbrella technique" provides continuous peripapillary ring-shaped histologic sections at varying diameters. In this study, we serially sectioned the processed tissue into 4-μm-thick ring sections, later identifying those ring sections having a precise diameter of 3.0, 3.5, 4.0, and 4.5 mm. Each of these four ring sections was photographed under the microscope at high resolution, and 100 equidistant RNFL thickness measurements around the circumference were taken. These RNFL thickness measurements were then plotted in a TSNIT anatomic orientation. The thickness data were also analyzed in four equally sized quadrants.

Statistical Analysis

RNFL thickness values are presented using descriptive statistics in micrometer units, means, and SD. Comparison of quadrants (temporal, superior, nasal, and inferior) was performed with ANOVA, controlling for multiple comparisons using the Bonferroni method. Differences of thickness change between rings of different diameters were performed

From the Department of Ophthalmology, Hadassah–Hebrew University Medical Center, Jerusalem, Israel.

Supported by Carl Zeiss Meditec (EZB).

Submitted for publication May 25, 2007; revised July 5 and August 29, 2007; accepted January 14, 2008.

Disclosure: **M.J. Cohen**, None; **E. Kaliner**, None; **S. Frenkel**, None; **M. Kogan**, None; **H. Miron**, None; **E.Z. Blumenthal**, Carl Zeiss Meditec (F)

The publication costs of this article were defrayed in part by page charge payment. This article must therefore be marked "*advertisement*" in accordance with 18 U.S.C. §1734 solely to indicate this fact.

Corresponding author: Eytan Z. Blumenthal, Department of Ophthalmology, Hadassah University Hospital, P.O. Box 12000, Jerusalem 91120, Israel; eytan@blumenthal.org.il.

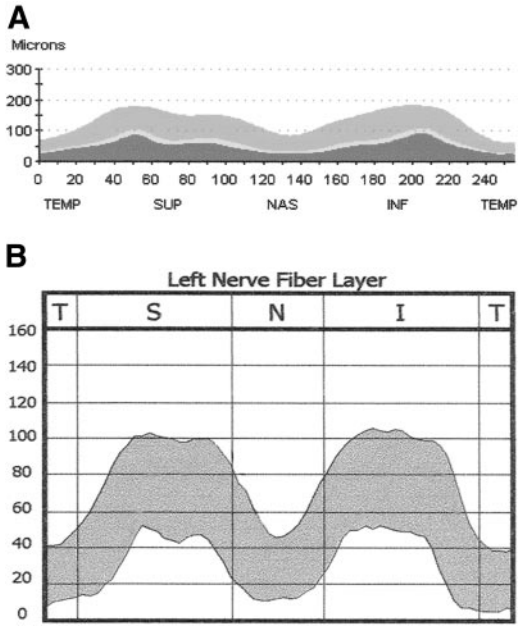

FIGURE 1. The normative database values for peripapillary RNFL thickness measured using (**A**) the Stratus OCT (at 3.4-mm diameter) and (**B**) the GDx-VCC (at 2.8–3.2-mm diameter), as presented on the standard printouts. Both show a double hump pattern along the TSNIT graph.

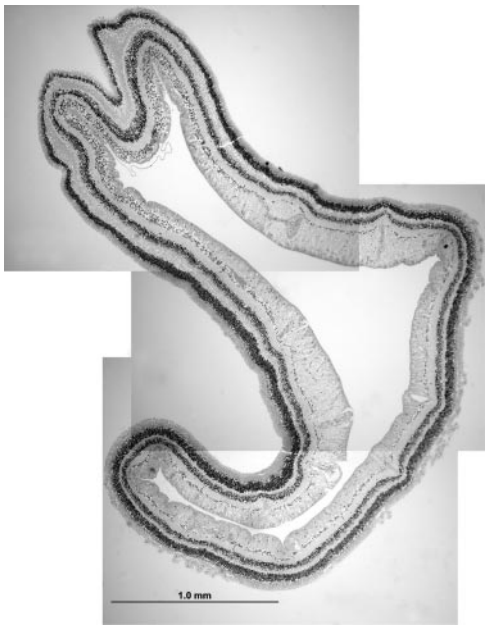

FIGURE 2. A representative ring section (subject 6, 3.5-mm diameter ring section) demonstrating a double-hump configuration (thickest RNFL seen superiorly and inferiorly).

using the Friedman two-way analysis of variance by ranks and the Page test for a monotonic trend for comparison for more than two matched values.[10] In all specimens, mean thickness was calculated for every single point of the 100 circumference points, providing 100 mean values for each ring diameter along its circumference. Mean values from adjacent rings were compared with paired analyses (3.0 vs. 3.5 mm, 3.5 vs. 4.0 mm, and 4.0 vs. 4.5 mm). Additionally, we examined the change of mean differences in diameter thickness at each point in the circumference using paired analyses.

RESULTS

Table 1 presents demographic characteristics, including cause of death and time to fixation, for the 17 subjects from whom postmortem eyes were obtained for this study. The specific causes of death, as listed in Table 1, are not expected to affect the retina or optic nerve in any particular way.

Figure 2 shows a representative 3.5-mm diameter peripapillary ring section (subject 6), demonstrating the thickness modulation changes observed along the TSNIT circumference. The data describing the percentage of RNFL in each quartile (Table 2) illustrate that though individual RNFL thickness measurements display an inverse association with their distance from the disc, the relative thickness distribution among the four quadrants remains conserved.

Figure 3A–D presents, for each of the four diameter rings (3.0 mm, 3.5 mm, 4.0 mm, and 4.5 mm) the average and range of RNFL thickness values along the peripapillary TSNIT ring. Significant variability is noted among the 17 normal eyes, more so at the superior and inferior regions.

We calculated the thickness differences among consecutive rings of 3.0-mm, 3.5-mm, 4.0-mm, and 4.5-mm diameter for

TABLE 1. Demographic Characteristics of Subjects from Whom Postmortem Eyes Were Obtained

Subject	Eye	Sex	Age (y)	Race	Time to Fixation (h)	Cause of Death
1	L	M	60	C	10.5	Coronary artery disease
2	R	F	67	C	7	Intracranial and subarachnoid hemorrhage
3	R	M	58	C	4.5	Myocardial infarction
4	L	M	64	A	7.5	Lung cancer
5	L	M	51	C	8	Glioblastoma without metastases
6	R	M	74	C	8	Myocardial infarction
7	L	M	68	C	6	Lung cancer
8	R	F	80	C	5	Unknown
9	L	F	73	C	3	Cancer
10	L	M	71	C	5	Cerebrovascular accident
11	R	F	59	C	3	Myocardial infarction
12	L	M	64	C	5	Motor vehicle accident trauma
13	R	F	66	C	6	Cardiac arrest
14	L	F	54	C	4.5	Intracranial hemorrhage
15	L	M	65	C	5	Lung cancer
16	L	M	52	C	6	Cardiac arrest
17	R	F	75	C	4	Myocardial infarction

L, left; R, right; M, male; F, female; C, Caucasian; A, African American.

TABLE 2. Mean RNFL Thickness (microns) in Each Quadrant, for Each Diameter Ring Section

	3.0 mm		3.5 mm		4.0 mm		4.5 mm	
Quadrant	**Mean ± SD**	**Area (%)**	**Mean ± SD**	**Area (%)**	**Mean ± SD**	**Area (%)**	**Mean ± SD**	**Area (%)**
Temporal	52.6 ± 23.5	19	49.2 ± 26.4	20	43 ± 21.3	20	38 ± 13	20
Superior	87.2 ± 33.3	31	75.3 ± 26.5	31	65.1 ± 16.6	30	57.5 ± 17	31
Nasal	57.5 ± 18	20	48.1 ± 15	20	42.8 ± 11.5	20	38.4 ± 10	20
Inferior	85.6 ± 30	30	69.4 ± 22.4	29	62.7 ± 18	30	54.7 ± 16.9	29
Overall	70.7 ± 22	100	60.3 ± 19.5	100	53.2 ± 18.5	100	47.1 ± 15	100

Data are presented as RNFL thickness and percentage of total cross-sectional area. Statistical analysis of the data using ANOVA, controlled for multiple comparisons, resulted in statistically significant differences in RNFL thickness between the following-quadrant pairs: superior-nasal, superior-temporal, inferior-nasal, inferior-temporal ($P < 0.01$). No statistically significant differences in RNFL thickness were found between the following pairs: superior-inferior, nasal-temporal.

each quadrant and for the mean ring thickness (Table 3). The difference between the mean of any two rings was highly significant ($P < 0.001$ for all pairwise comparisons).

We analyzed statistically the incremental change between any two consecutive rings (Table 3). This incremental change observed was larger for smaller consecutive rings, as opposed to relatively larger consecutive rings.

DISCUSSION

In this study, data are provided on the RNFL thickness modulation in concentric peripapillary ring sections centered on the optic disc. Few studies have previously analyzed healthy human eye RNFL thickness data and have limited their analysis to only a few measurement points along the peripapillary circumference.[1]

It is important to acknowledge, in the context of this work, that histologic data on human eyes have several inherent limitations that cannot be reliably controlled. These limitations include the changes that any living tissue undergoes after severe ischemia, death, fixation, embedding, and staining.[1] Although this is a criticism of any histologic attempt to quantify RNFL,[3–8] it is reasonable that analyzing and quantifying the actual RNFL tissue can indeed produce valuable information, complementing indirect approaches, be it observation, imaging, or any other in vivo assessment. In a study of RNFL modulation around the optic disc, it is expected that any postmortem histologic tissue changes would likely occur relatively uniformly across the tissue. Hence, RNFL modulation would be relatively resistant to these changes, unlike absolute thickness parameters.

The existence of the double hump pattern of the peripapillary RNFL, as perceived on imaging, has been supported by limited histologic data derived from healthy human eyes. We measured RNFL thickness using a well-defined histologic pro-

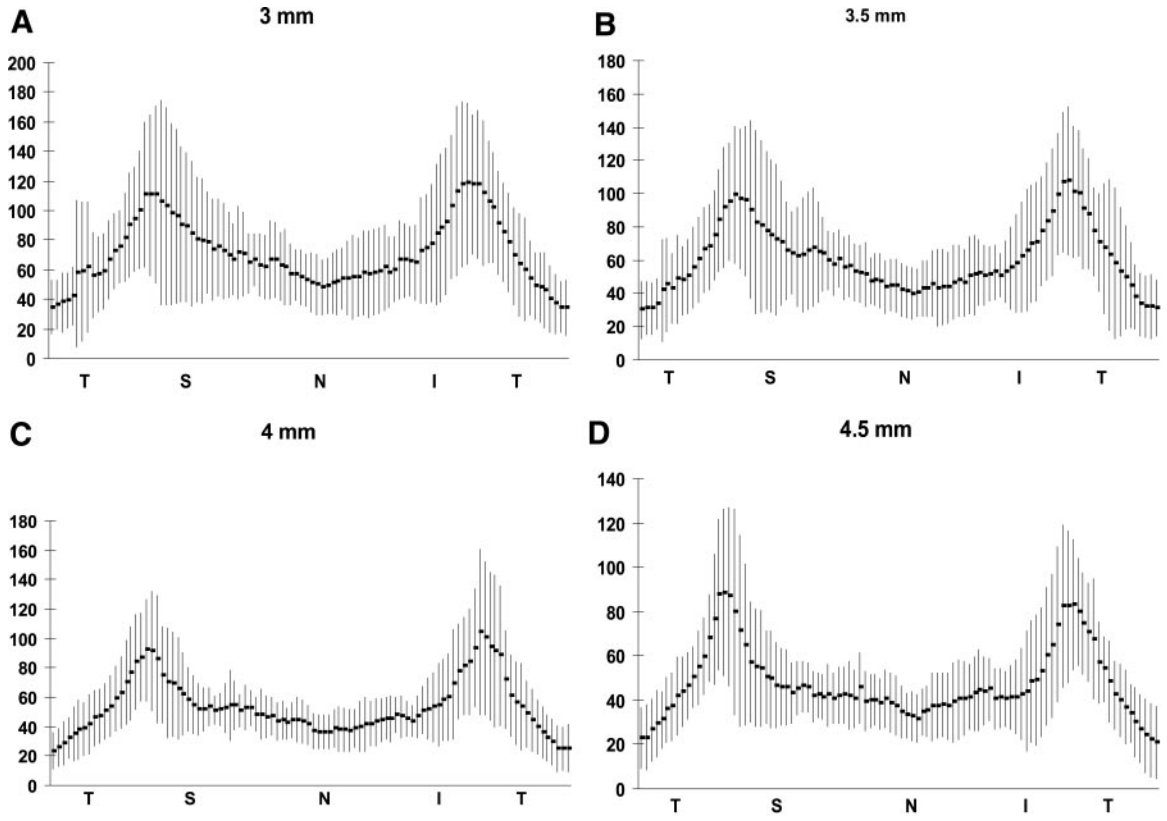

FIGURE 3. **(A–D)** For each of the four diameter rings, 100 thickness data points are plotted along the TSNIT circumference. For each data point, mean (*dark point*) ± 2 SD thickness is shown in microns.

TABLE 3. Thickness Decreases with Increase in Ring Size

Quadrant	3.0 vs. 3.5 mm	3.5 vs. 4.0 mm	4.0 vs. 4.5 mm	ANOVA*	Trend†
Temporal	5.6 ± 4.13	6.25 ± 2.6	2.5 ± 1.7	<0.001	0.002
Superior	11.3 ± 4.7	10.4 ± 3.4	7.9 ± 4.8	0.077	0.012
Nasal	10.3 ± 2.4	4.9 ± 2	3.9 ± 1.5	<0.001	<0.001
Inferior	14.6 ± 8.2	6.4 ± 4	10 ± 5.7	<0.001	<0.001

Shown are absolute differences in RNFL thickness (microns) between adjacent risk diameters, per quadrant and overall values (mean ± SD).

* Friedman's two-way ANOVA *P* for the RNFL thickness change found between the 3.0-mm vs. 3.5-mm and the 4.0-mm vs. 4.5-mm diameter rings.

† Page's test for trend *P* value for the RNFL thickness change found between the 3.0-mm vs. 3.5-mm vs. 4.0-mm vs. 4.5-mm diameter rings.

cessing approach (formalin-fixed, paraffin-embedded, and hematoxylin-eosin–stained light microscopy tissue sections).[9] The uniqueness of this study relates to the fact that a sizable number of eyes were measured in a standardized, systematic fashion, obtaining high-resolution grids of peripapillary ring sections, all centered on the optic disc. The order of data resolution obtainable using this technique was over a magnitude larger than previously obtainable.[1] Consequently, this study provides, for the very first time, an attempt to define a high-resolution map of the normative range for RNFL thickness in healthy human eyes processed histologically.

Quantitative discrepancies can be noted when comparing OCT against SLP normative database–averaged thickness values and when comparing these imaging data sets to the histologically derived data set presented in this study. Figures 1 and 3 enable a comparison of imaging with histology thickness data, extracted from equivalent diameter rings. For an OCT histology comparison, Figure 1A (ring diameter, 3.4 mm) should be compared with Figure 3B (ring diameter, 3.5 mm). This comparison demonstrates superior and inferior peaks of roughly equivalent thickness (approximately 100 μm) in the OCT and the histology data. Both sets of data suggest a split superior bundle in the pooled normative data, as previously demonstrated.[11] For a SLP histology comparison, Figure 1B (ring diameter, 2.8–3.2 mm) should be compared with Figure 3A (ring diameter, 3.0 mm). When viewing these two figures, the RNFL thicknesses were different, whereas the overall pattern was maintained.

It is important to note that though the qualitative shape of the peripapillary RNFL thickness modulation can be compared across these different modalities, the quantitative comparison of actual thickness values is of little value because of the many artifacts in imaging and histologic evaluation of the RNFL.[9,11] A surprising twofold thickness difference was recently found when OCT and SLP absolute thickness values were compared on the same group of healthy persons.[12] Moreover, the equation enabling the transformation of retardation values to RNFL thickness microns used in SLP has originated from a study on two postmortem monkey eyes that were scanned using a prototype SLP device and later subjected to histologic processing and RNFL thickness measurements.[13]

RNFL thickness modulation relates to the qualitative pattern observed along each peripapillary circumference. It relates to the relative thickness changes along the TSNIT path rather than to absolute thickness values. Our histologic modulation findings are in alignment with known modulation patterns for both OCT and SLP (Fig. 1).

In contrast to the modulation patterns found, the actual thickness values demonstrate significant differences between histology and imaging and significant differences between OCT and SLP.[12]

In this study we chose the smallest ring section to be 3 mm in diameter given that smaller rings are difficult to obtain consistently using the umbrella method, partly because of a gradual formation of perpendicularity of the retina very close to the disc margin in the closed-funnel configuration obtained. We chose the 4.5-mm diameter ring as the largest diameter because, clinically, RNFL thickness outside 1 disc diameter from the edge of the disc is not routinely evaluated by imaging devices.

Acknowledgments

Tissue used in this study was procured from the National Disease Research Interchange.

References

1. Frenkel S, Morgan JE, Blumenthal EZ. Histological measurement of retinal nerve fibre layer thickness. *Eye*. 2005;19:491–498.
2. Essock EA, Sinai MJ, Fechtner RD, Srinivasan N, Bryant FD. Fourier analysis of nerve fiber layer measurements from scanning laser polarimetry in glaucoma: emphasizing shape characteristics of the 'double-hump' pattern. *J Glaucoma*. 2000;9:444–452.
3. Varma R, Skaf M, Barron E. Retinal nerve fiber layer thickness in normal human eyes. *Ophthalmology*. 1996;103:2114–2119.
4. Dichtl A, Jonas JB, Naumann GO. Retinal nerve fiber layer thickness in human eyes. *Graefes Arch Clin Exp Ophthalmol*. 1999; 237:474–479.
5. Radius RL. Thickness of the retinal nerve fiber layer in primate eyes. *Arch Ophthalmol*. 1980;98:1625–1629.
6. Quigley HA, Addicks EM. Quantitative studies of retinal nerve fiber layer defects. *Arch Ophthalmol*. 1982;100:807–814.
7. Ogden TE. Nerve fiber layer of the primate retina: thickness and glial content. *Vision Res*. 1983;23:581–587.
8. Morgan JE, Waldock A, Jeffery G, Cowey A. Retinal nerve fibre layer polarimetry: histological and clinical comparison. *Br J Ophthalmol*. 1998;82:684–690.
9. Blumenthal EZ. Quantifying retinal nerve fiber layer thickness histologically: a novel approach to sectioning of the retina. *Invest Ophthalmol Vis Sci*. 2004;45:1404–1409.
10. Siegel S, Castellan NJ. *Nonparametric Statistics for the Behavioral Sciences*. New York: McGraw-Hill; 1988.
11. Kaliner E, Cohen MJ, Miron H, Kogan M, Blumenthal EZ. Retinal nerve fiber layer split bundles are true anatomic variants. *Ophthalmology*. 2007;114:2259–2264.
12. Leung CK, Chan WM, Chong KK, et al. Comparative study of retinal nerve fiber layer measurement by StratusOCT and GDx VCC, I: correlation analysis in glaucoma. *Invest Ophthalmol Vis Sci*. 2005;46:3214–3220.
13. Weinreb RN, Dreher AW, Coleman A, et al. Histopathologic validation of Fourier-ellipsometry measurements of retinal nerve fiber layer thickness. *Arch Ophthalmol*. 1990;108:557–560.